Краткие сообщения ОИЯИ №4[67]-94 *JINR Rapid Communications No.4[67]-94*
УДК 539.17:621.384.63

THE NUCLOTRON INTERNAL TARGETS*

A.S.Artiomov

The peculiarities of the nucleus-internal target interaction at the synchrotrons are theoretically investigated. Taking this interaction into account, analytical expressions for luminosities averaged over cycle time, time evolution of the current, transverse and longitudinal emittances are obtained. The graphical functions, characterizing the luminosities and parameter evolution of a *d*, C and Ar nucleus beam with energies of 1 and 6 AGeV for different internal targets at the Nuclotron are presented.

The investigation has been performed at the Laboratory of High Energies, JINR.

Внутренние мишени в нуклотроне

А.С.Артемов

Теоретически исследованы особенности взаимодействия ядер с внутренними мишенями в синхротронах. С учетом этого взаимодействия получены аналитические выражения для усредненных за время цикла светимостей, временной эволюции тока пучка, его поперечного и продольного эмиттансов. Графические зависимости, характеризующие светимости и эволюцию параметров пучка ядер *d*, С и Ar с энергиями 1 и 6 АГэВ,представлены для различных внутренних мишений в нуклотроне.

Работа выполнена в Лаборатории высоких энергий ОИЯИ.

1. Introduction

Relativistic nuclear physics deals with the study of processes in which the constituents of nuclear matter move with relative velocities close to the velocity of light. The asymptotic character of such natural phenomena has played a decisive role in a constraction of the Nuclotron, a strong superconducting accelerator of relativistic nuclei at the LHE of the Joint Institute for Nuclear Research in Dubna [1]. As the first experiments [2,3] showed, this accelerator provides good possibilities for internal target technique. The planning of internal target experiments requires a detailed knowledge of the

*Report at the Workshop on Perspectives of Relativistic Nuclear Physics, May 31 — June 5, 1994, Varna, Bulgaria

ion-target interaction. This interaction is sufficiently well studied for the light ion beams circulating into the synchrotrons (see, for example, [4—7]). As shown in this report, for more heavy ions some peculiarities of the ion-internal target interaction take place. Taking this interaction into account, the luminosities averaged over cycle time and parameter evolution of d, C and Ar nucleus beam with energies of 1 and 6 AGeV for different internal targets at the Nuclotron are investigated.

2. Beam-Internal Target Interaction at the Synchrotrons and Evolution of an Ion Beam Parameters

Physics experiments with internal targets are usually realized in recirculation mode of synchrotron operation after beam injection and acceleration. It is important for this mode of operation that the mean energy loss of ions per target traversal is compensated by an appropriate synchrotron acceleration in the rf-cavity. If we suppose that ions traverse a homogeneous target every turn and residual gas effects are negligible, general analytical expressions for beam parameter evolution can be obtained.

Small angle scattering and energy loss straggling of ions lead to the growth of transverse and longitudinal beam emittances. For a sufficiently large number of target traversals it can be described by the following equation [7,8]

$$\varepsilon_i^{(N)}(\eta) = \varepsilon_i^{(0)} + 0.5N\beta_i\eta^2\overline{(\delta Y')^2} + \\ + 0{,}5N\eta^2[\gamma_i D_i^2 + 2\alpha_i D_i D_i' + \beta_i (D_i')^2]\,\overline{\delta^2}, \qquad (1)$$

$$\varepsilon_l^{(N)}(\eta) = \varepsilon_l^{(0)} + 0.5N\beta_l\eta^2\delta^2. \qquad (2)$$

Here $\varepsilon_i^{(0)}$, $\varepsilon_i^{(N)}$ are the initial and after N target traversals horizontal ($i = x$) or vertical ($i = z$) transverse emittances corresponding to η standard deviations in the Gaussian distribution; $\varepsilon_l^{(0)}$ and $\varepsilon_l^{(N)}$ are analogous longitudinal emittances; β_i, α_i, D_i, D_i', $\gamma_i = (1 + \alpha_i^2)/\beta_i$ are the parameters of the accelerator at the target location; $\overline{(\delta Y')^2}$ and $\overline{\delta^2}$ are the mean square deviations in angle and relative momentum after target traversal; $\beta_l = (\omega_{rf}/\omega_s) \times \sqrt{(|\zeta|\, 2\pi p\beta c)/(ZU\cos\varphi_s)}$; ω_{rf} and ω_s are the frequences of rf-cavity and synchronous particle turn, respectively; $\zeta = \delta\,(\Delta\omega/\omega)$ is the longitudinal

dispersion of the accelerator; U is the voltage amplitude of rf-cavity; φ_s is the phase of the synchronous particle; $p, \beta c$ and Z are the momentum, velocity and charge number of ions respectively. Using Moliere's approximation of the screened coulomb potential of the Thomas-Fermi atom and the Landau-like energy loss distribution, for relativistic nuclear-thin target interaction we obtain

$$\overline{(\delta Y')^2} \approx 2\cdot 10^{-7}\, t A_0^{-1} \left(\frac{ZZ_0}{A\gamma\beta^2}\right)^2 \left(\ln\left(\frac{\theta_{cm}}{\theta_m}\right) - 0.5\right) = \\ = t\cdot f_1(Z, A, Z_0, A_0, \beta), \qquad (3)$$

$$\overline{\delta^2} \approx 2\cdot 10^{-7}\, t \frac{Z_0}{A_0}\left(\frac{Z}{\beta^2 A}\right)^2 \left(1 - \frac{\beta^2}{2}\right) = t\cdot f_2(Z, A, Z_0, A_0, \beta). \qquad (4)$$

Here $\gamma = (1-\beta^2)^{-0.5}$; t is the target thickness [g/cm^2]; A, Z_0 and A_0 are the nuclear mass number, charge and mass number of the target, respectively; $\theta_m \approx 4.8\cdot 10^{-6} Z_0^{1/3} \sqrt{1 + 1.77\cdot 10^{-4}(ZZ_0/\beta)^2}/(\beta\gamma A)$ is Moliere's screening angle; $\theta_{cm} \approx 0.15[1 + 1.53\cdot 10^{-2}(ZZ_0/\beta)]\cdot[\beta\gamma A(A^{1/3}+A_0^{1/3})]^{-1}$ is the maximum angle of the Rutherford scattering determined by the nuclear radii of target and projectile. As an example, Fig.1 shows the $f_1(\,)$ and $f_2(\,)$ curves characterizing the transverse emittance growth of the d, C and

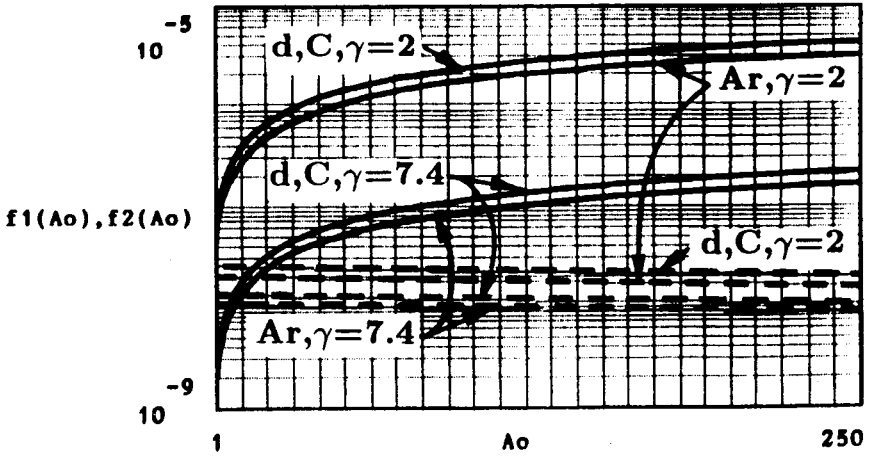

Fig.1. The f_1 (solid line) and f_2 (dashed line) functions vs target mass number A_0 for different incident nuclei

Ar nucleus beam with $\gamma = 2$ and 7.4 for different internal targets. The growth of beam emittances, inelastic nuclear scattering and large angle elastic scattering in a single projectile passage through the target lead to beam losses. If we take into account only the first channel, the time evolution for circulating beam intensity (in relative units) can be obtained from the Fokker-Planck model of projectile diffustion in the (Y_i', Y_i)-phase spaces [9]. As the longitudinal emittance growth can be influenced by the rf-cavity voltage (see eq. (2)), we suppose that particle losses in the longitudinal phase space can be made negligible. Using the results of ref. [10], the probability of projectile loss because of diffusion in a beam after N target traversals is estimated by $P(N) = \prod_{i=x,z} P_i(\varepsilon_i^{(N)})$, where calculated $P_i(\varepsilon_i^{(N)})$-function is shown in Fig.2. Approximating this function by $\exp[-5.36(s_i - 0.06)]$, the effective cross section σ_i of projectile loss after start time τ_i can be obtained as

$$\sigma_i \approx 2.2 \cdot 10^{-24} \frac{A_0}{A_i} [\beta_i f_1() + f_2() (\gamma_i D_i^2 + 2\alpha_i D_i D_i' + \beta_i (D_i')^2], \qquad (5)$$

$$\tau_i \approx \frac{2S\,(0.12 A_i \eta^2 - \varepsilon_i^{(0)})}{t\eta^2 \beta c} \times$$

$$\times [\beta_i f_1( ) + f_2( ) (\gamma_i D_i^2 + 2\alpha_i D_i D_i' + \beta_i (D_i')^2)]^{-1} \equiv \frac{S}{t\beta c}\, ai(), \qquad (6)$$

where S, A_i are the ring circumference and acceptance.

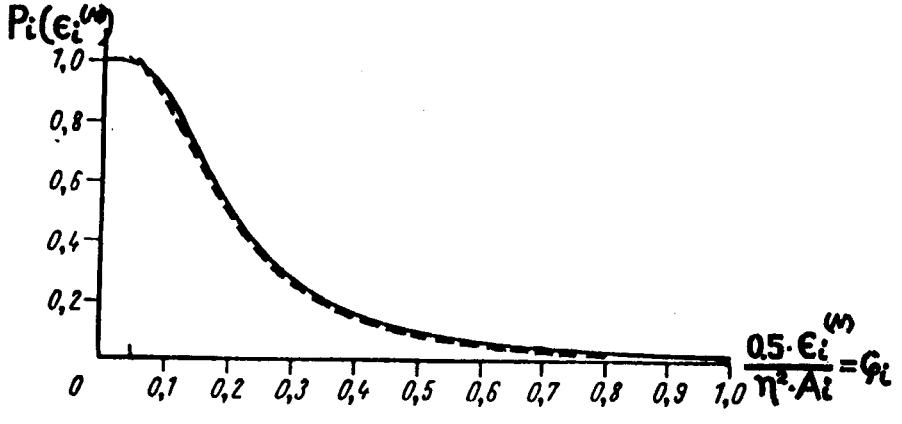

Fig.2. The probability of diffusion particle loss in (Y_i', Y_i)-phase space for the beam with transverse emittance $\varepsilon_i^{(N)}$, the dashed line shows the $\exp[-5.36(s_i - 0.06)]$ approximation

Inelastic nuclear interaction and large angle elastic scattering lead to the projectile loss in every passage through the target with the cross section

$$\sigma_t = \sigma_c f() + 0.5\sigma_{in}\,[4 - erf(\theta_{xa}/2\theta_d) - erf(\theta_{za}/2\theta_d)]. \qquad (7)$$

Here $f() \equiv 0.5\,(\theta_{xa}^{-2} + \theta_{za}^{-2} - 2\theta_{cm}^{-2})$, $\theta_{ia}^2 \approx A_i/(\beta_i \pi)$ $(i = x, z)$, $\theta_d \approx$ $\approx 0.15[A(\gamma^2 - 1)^{0.5}\,(A^{1/3} + A_0^{1/3})]^{-1}$, $\sigma_{in} \approx 6 \cdot 10^{-26}(A^{1/3} + A_0^{1/3})^2$, $\sigma_c \approx$ $\approx 3 \cdot 10^{-31}\,[Z_0 Z/(\beta^2 \gamma A)]^2$ and Gaussian approximation of a central maximum of plane diffractional nuclear scattering is used. In eq.(7) we should assume $\theta_{ia} = \theta_{cm}$, when $\theta_{ia} > \theta_{cm}$. Depending on the collision energy and the type of colliding nuclei, different terms dominate in σ_t. The average beam lifetime (T_b) and cross section of the projectile loss (σ_{loss}) can be estimated as

$$T_b \approx \frac{a + \sum\limits_i \tau_i \sigma_i b_i}{\sigma_t + \sum\limits_i b_i \sigma_i}, \quad (i = x, z), \qquad (8)$$

$$\sigma_{\text{loss}} = \sigma_t + \sigma_{\text{ef}} = a/T_b, \qquad (9)$$

where $a = A_0 S/(6 \cdot 10^{23} t\beta c)$, $b_i = 1$ if $\tau_i < T = a/\sigma_t \equiv \bar{t}() \; S/(t\beta c)$ and $b_i = 0$ otherwise, σ_{ef} is the effective cross section of the diffusion projectile loss.

The luminosity is the product of beam current and target thickness averaged over time. In recirculation mode of the accelerator run the luminosity L_c averaged over the cycle time T_c has the maximum value of $L_c = N_0/(T_c \sigma_{\text{loss}})$ (N_0 is the number of the circulating particles before beam-target interaction) which is independent of target thickness when $t \geq t_c = = A_0 S/(6 \cdot 10^{23}\, T_c \beta c \sigma_{\text{loss}})$. For internal target thickness $t < t_c$ the luminosity is decreased by the value of t/t_c.

3. Internal Target Effects at the Nuclotron

Using the above results, the numerical calculations of internal target effects for d, C and Ar nuclei with energies of 1 and 6 AGeV are obtained at the Nuclotron $A_i \approx 40\pi$ mm·mrad, $\varepsilon_i^{(0)} \approx 2\pi$ mm· mrad, $\beta_i \approx 780$ cm,

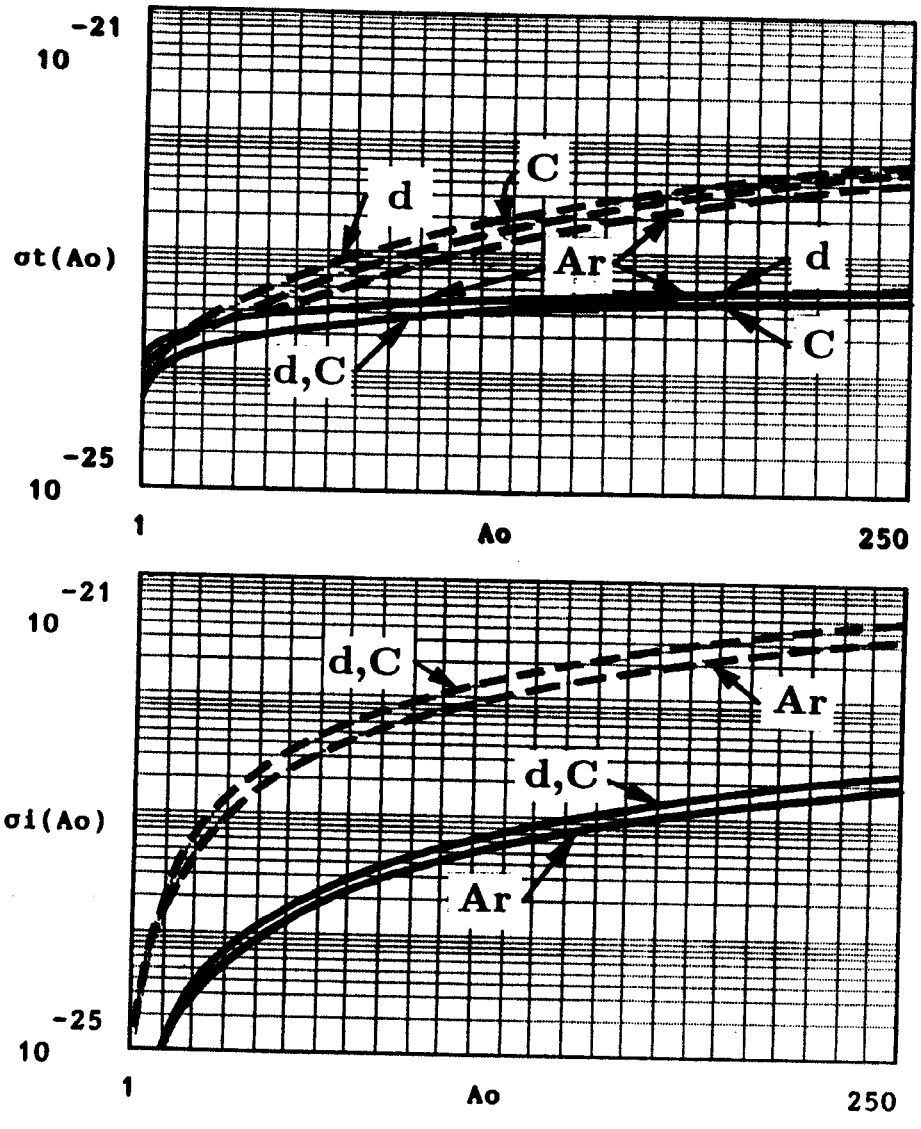

Fig.3. The σ_t and σ_i cross sections of the loss of relativistic d, C and Ar nuclei at the Nuclotron vs target mass number A_0 (– – 1 AGeV, —— 6 AGeV)

$|\alpha_i| \approx 1.3$, $D_i \approx 220$ cm, $D_i' \approx 0.3$ at the target location). Effective cross section of the diffusion particle loss $\sigma_i (i = x, z)$ and σ_t as a function of the target mass number A_0 are shown in Fig.3. The values of the $f()$-function (see Fig.4) in eq.(7) show that for high energy heavy projectiles at the

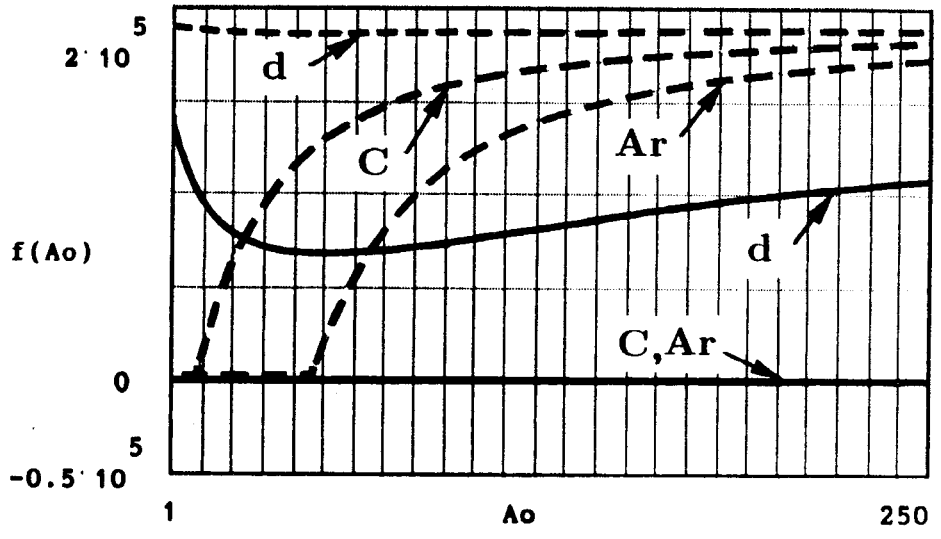

Fig.4. The $f()$-function in σ_t vs target mass number A_0 for different incident nuclei at the Nuclotron (– – 1 AGeV, —— 6 AGeV)

Nuclotron (for example, C and Ar nuclei with $\gamma = 7.4$) large angle coulomb scattering does not make contribution to σ_t. When the initial beam emittances ($\varepsilon_i^{(0)}$) are known, the corresponding values of T, τ_i and T_b can be obtained from Fig.3 and eqs.(6), (8). Correlation between τ_i and T is defined by the $ai()$ and $\bar{t}()$ functions, which are plotted in Fig.5. The presented in Figs.3,5 results show the substantial contribution of the diffusion process (related to small angle scattering in the target) to the losses (σ_{loss}) of the low energy relativistic projectiles. As the energy increases the area of A_0, where this contribution is negligible, is grown by including larger mass numbers of the target. The maximum values of luminosities averaged over cycle time per one projectile at the first stage of Nuclotron run (T_c= 10 s) are plotted in Fig.6. As the internal target thickness t[g/cm^2] is known ($t > t_c$) and using the presented in Fig.7 graphical functions of $T_b \cdot t$, the beam lifetime T_b [s] can be estimated. Assuming $T_b = T_c$ in the value of $T_b \cdot t$-function the target thickness of t_c can be also obtained.

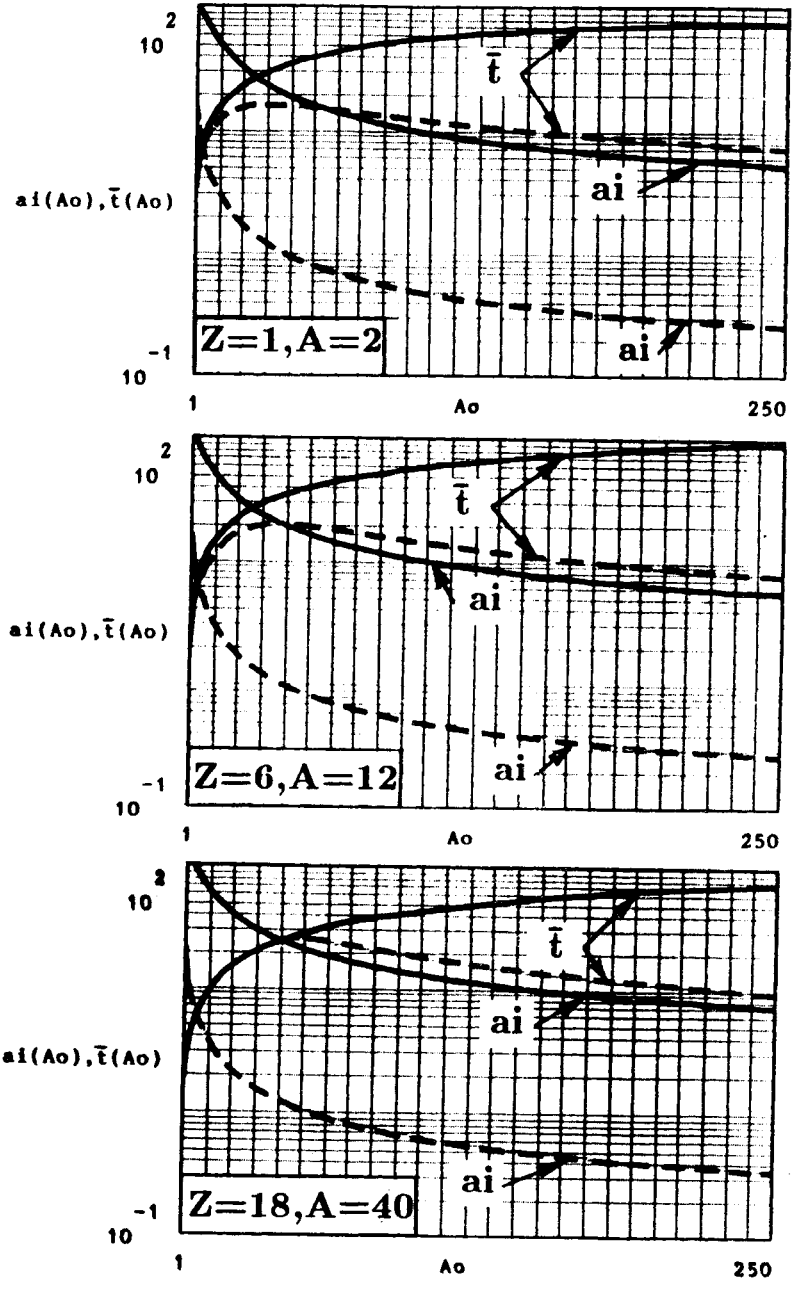

Fig.5. The *ai*() and $\bar{t}$() functions vs target mass number A_0 for different incident nuclei (– – 1 AGeV, —— 6 AGeV)

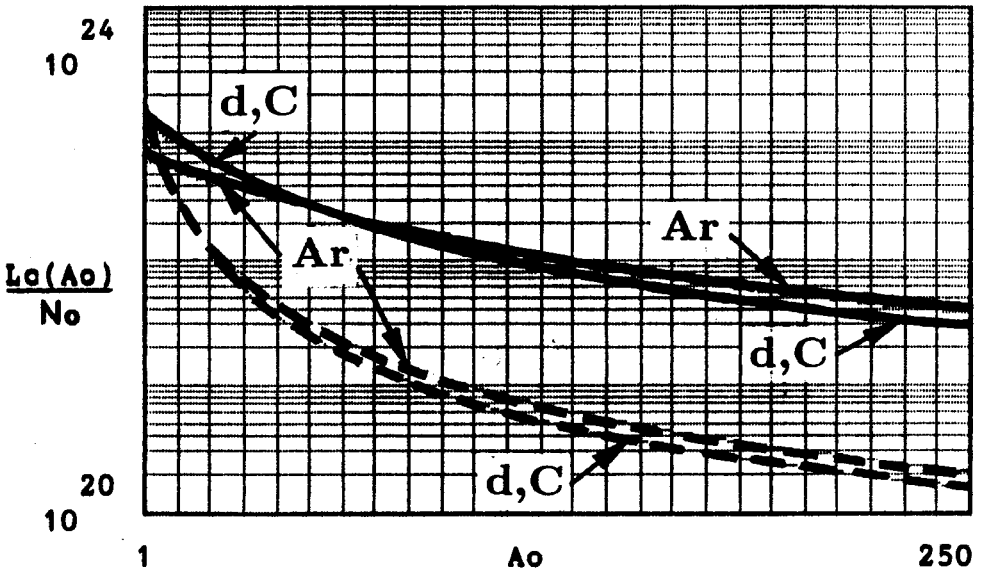

Fig.6. The maximum values of luminosities averaged over cycle time per one projectile (d, C and Ar nulcei) for different internal targets at the Nuclotron (T_c = 10 s, – – 1 AGeV, —— 6 AGeV)

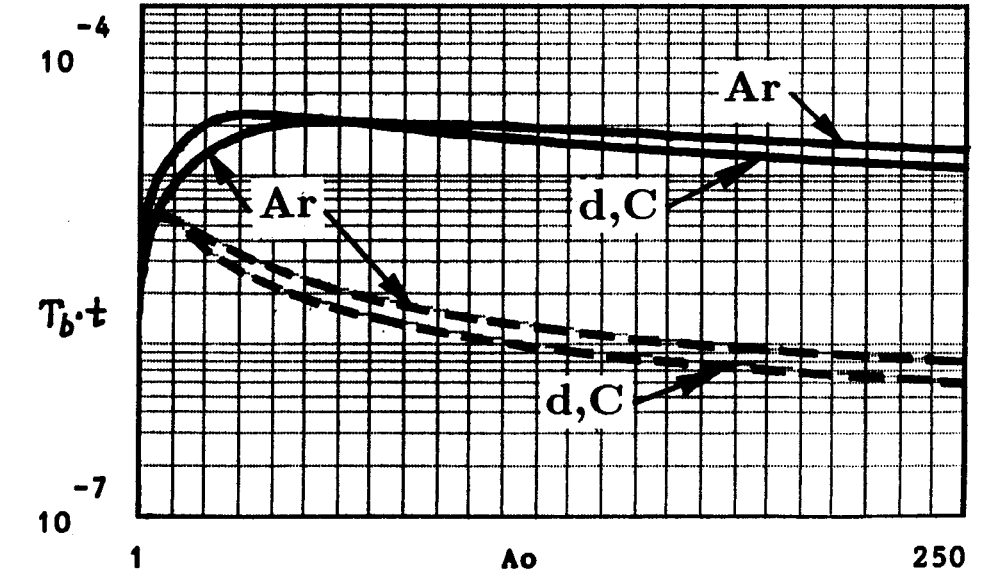

Fig.7. The $T_b \cdot t$-functions vs target mass number A_0 for different incident nuclei at the Nuclotron (– – 1 AGeV, —— 6 AGeV)

References

1. Baldin A.M. — JINR Communication E1-92-487, Dubna, 1992.
2. Baldin A.M. et al. — JINR Rapid Communications, No.4[61]-93, Dubna, 1993, p.13.
3. Baldin A.M. et al. — JINR Rapid Communications, No.2[65]-94, Dubna, 1994, p.26.
4. Hinterberger F., Mayer-Kuckuk T., Prasuhn D. — Nucl. Instr. and Meth. A, 1989, vol.275, p.239.
5. Noda K., Noda A., Katayama I., Sakamoto N. — Nucl. Instr. and Meth. A, 1991, vol.303, p.215.
6. Tschalar C. — Nucl. Instr. and Meth. A, 1991, vol.308, p.471.
7. Hinterberger F., Prasuhn D. — Nucl. Instr. and Meth. A, 1992, vol.321, p.453.
8. Artiomov A.S. — JINR Rapid Communications, No.4[61]-93, Dubna, 1993, p.6.
9. Bruck H. — Accelerateurs circulaires de particules, Paris: Presses Universitaires de France, 1966.
10. Hinterberger F., Prasuhn D. — Nucl. Instr. and Meth. A, 1989, vol.279, p.413.

Received on July 26, 1994.